






 Cite this: *RSC Adv.*, 2024, 14, 9758

# Novel mono substituted pyridoimidazoisoquinoliniums *via* a silver-catalyzed intramolecular cyclization and their applications in cellular imaging†

 Masato Kawakubo, Yoshikazu Inoh, Yuki Murata,  Mio Matsumura, \*  
Tadahide Furuno \* and Shuji Yasuike 

Cationic heterocycles, an important class of organic compounds soluble in polar solvents, have been gaining attention in the construction of fluorescent probes. This paper reports the quick synthesis of novel pyrido[1',2';2,3]imidazo[5,1-a]isoquinoliniums starting from 2-(2-ethynylphenyl)imidazo[1,2-a]pyridines at room temperature *via* intramolecular cyclization by employing a catalytic amount of silver trifluoromethanesulfonate in addition to lithium trifluoromethanesulfonate and silica gel as the counter anion source and additive, respectively. The designed pyridoimidazoisoquinoliniums consisted of an imidazo[1,2-a]pyridine fused isoquinolinium. The X-ray diffraction results revealed that pyrido[1',2';2,3]imidazo[5,1-a]isoquinolinium trifluoromethanesulfonate contained considerable planar parent skeletons and interacted by  $\pi$ - $\pi$  stacking with neighbouring molecules. Furthermore, in a methanol solution the designed 6-phenyl derivative exhibited strong fluorescence in the 420–450 nm region in addition to strong mitochondrial specificity in a cell staining assay.

 Received 17th February 2024  
Accepted 13th March 2024

DOI: 10.1039/d4ra01210k

[rsc.li/rsc-advances](https://rsc.li/rsc-advances)

## Introduction

Fluorescence bioimaging has been gaining significant attention, as a powerful tool for the visualization of specific organelles in live cells, since it enables the monitoring of biological activities and consequently helps in disease diagnosis.<sup>1–3</sup> Organic fluorescent dyes have been used to enhance the contrast for the imaging of biological specimens.<sup>4–10</sup> Consequently, several studies have investigated the design of organelle-targeted probes. Charged polycyclic heteroarenes, characterized by both fluorescence properties stemming from their  $\pi$ -conjugated skeletons and high solubilities attributed to their ionic structures, have been gaining significant attention. However, the majority of charged polycyclic heteroarenes with three or more condensed rings reported so far possess a benzene-fused quinolinium, quinolizinium, or cinnolinium skeleton, indicating a notable lack of structural diversity. Only a few studies have reported the application of cationic fluorophores fused with two or more heteroaromatic compounds in intercellular imaging (Fig. 1).

Vaquero *et al.* reported the synthesis and properties of fluorescent DNA probes consisting of benzocinnolinium fused imidazo[1,5-*a*]pyridine (**I**)<sup>11,12</sup> and pyridazinium fused benzimidazole (**II**).<sup>13</sup> Maheswari *et al.* reported the application of a synthesised azafluoranthemium including cinnolinium and indazole (**III**) in mitochondrial visualization in living cells.<sup>14</sup> You *et al.* reported that aza[4]helicenes, pyrrolo[3,2-*k*]phenanthridiziniums exhibited fluorescence in the acidic environment of lysosomes.<sup>15</sup> Our group has recently reported the synthesis of pyrido[1',2';2,3]imidazo[5,1-*a*]isoquinoliniums consisting of imidazo[1,2-*a*]pyridine and isoquinolium.<sup>16</sup> The designed isoquinoliums were successfully employed in the intracellular imaging of the endoplasmic reticulum in particular.<sup>17</sup> However, only a few approaches have been proposed for the synthesis of pyrido[1',2';2,3]imidazo[5,1-*a*]

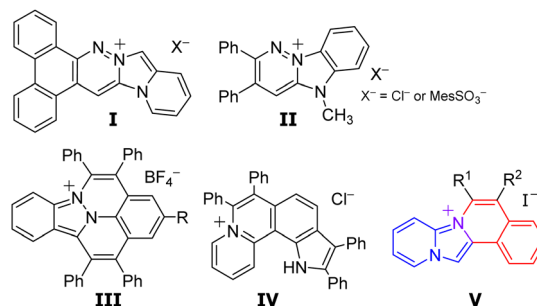


Fig. 1 Cationic fluorophores fused heteroaromatic rings.

School of Pharmaceutical Sciences, Aichi Gakuin University, 1-100 Kusumoto-cho, Chikusa-ku, Nagoya 464-8650, Japan. E-mail: m-matsu@dpc.agu.ac.jp; furuno@dpc.agu.ac.jp

† Electronic supplementary information (ESI) available. CCDC 2324904. For ESI and crystallographic data in CIF or other electronic format see DOI: <https://doi.org/10.1039/d4ra01210k>

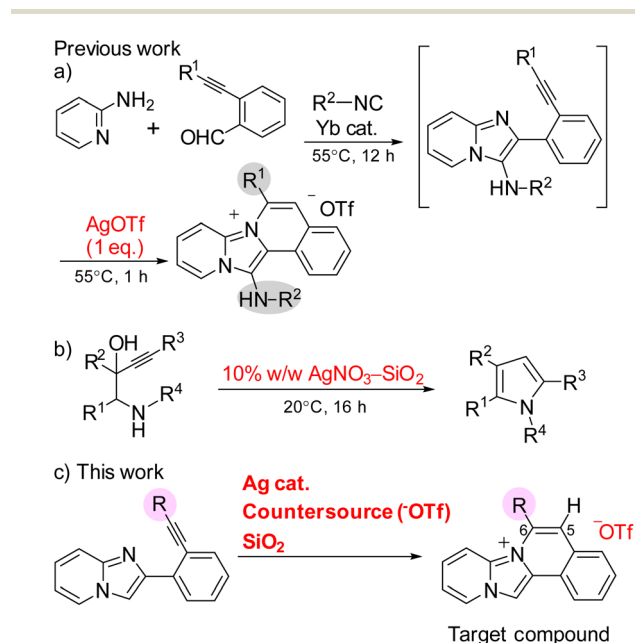


isoquinoliniums.<sup>16–19</sup> Furthermore, the properties of their derivatives and applications are still ambiguous.

The intermolecular nucleophilic cyclization of alkynes with a nitrogen-functional side chain mediated by silver complexes is a facile and powerful method for the synthesis of key heterocycles.<sup>20–23</sup> Zhou *et al.* conducted the synthesis of 13-aminopyrido[1',2';2,3]imidazo[5,1-*a*]isoquinoliniums by the Ag-mediated three-component domino reaction of 2-alkynylbenzaldehydes, 2-aminopyridines, and isocyanides at 55 °C (Scheme 1a).<sup>18</sup> However, the cyclization reaction required stoichiometric amounts of silver(i) trifluoromethanesulfonate (AgOTf) because the trifluoromethanesulfonate also acted as a counter anion for the products, limiting the application of their synthetic method. Knight and coworkers discovered that various 3-alkynyl-hydroxyalkanamine derivatives can undergo nucleophilic cyclizations to provide the corresponding pyrroles using catalytic amount of 10% w/w AgNO<sub>3</sub>-SiO<sub>2</sub> (Scheme 1b).<sup>24</sup> This 5-*endo-dig* cyclization was promoted by a silver catalyst supported on a silica gel and required 16 h under mild conditions. Consequently, this study reported the rapid synthesis of pyrido[1',2';2,3]imidazo[5,1-*a*]isoquinoliniums at room temperature *via* the silver-catalysed nucleophilic cyclization of 2-ethynylphenylimidazopyridine with lithium trifluoromethanesulfonate (LiOTf) and silica gel as the counter anion source and additive, respectively (Scheme 1c). The obtained compounds were characterized by different spectroscopic techniques and their application in cell imaging was also investigated.

## Results and discussion

The cyclization precursors, 2-(2-ethynylphenyl)imidazo[1,2-*a*]pyridines **1**, were easily synthesised by the Sonogashira cross-coupling reaction between 2-(2-iodophenyl)imidazo[1,2-*a*]

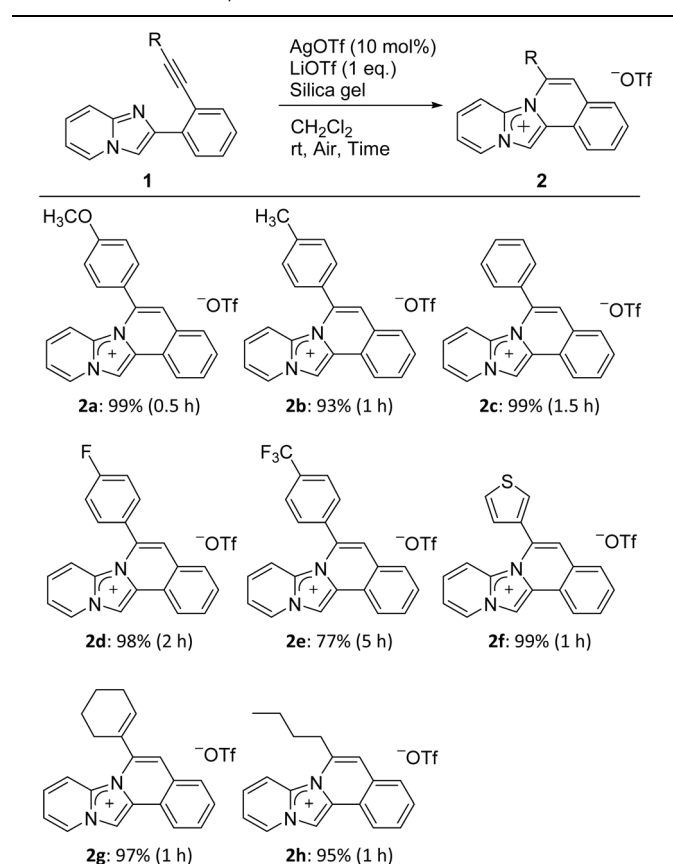


**Scheme 1** Ag-mediated intermolecular nucleophilic cyclization of alkynes with nitrogen-functional side chain.

pyridine and various terminal acetylenes.<sup>16</sup> These precursors were then treated with AgOTf (10 mol%) as the Lewis acid, LiOTf (1 equiv.) as the counter anion source, and silica gel (99 : 1 w/w *vs.* AgOTf) as the additive under aerobic conditions in CH<sub>2</sub>Cl<sub>2</sub> at room temperature (Table 1). All reactions followed the 6-*endo*-diagonal type to give the desired ring-closure products **2a–h** in good to excellent yields. Precursors **1a–d** bearing electron donors or halide groups on the terminal benzene ring provided the corresponding products **2a–d** in a short reaction time and high yields. On the other hand, **2e** was obtained in a lower yield and required longer reaction times due to the stronger electron-withdrawing trifluoromethyl group of **1e**. Furthermore, ethynylimidazopyridines **1f–h** with a heterocyclic thiophene, vinyl, or alkyl group, respectively, afforded the respective products **2f–h** within one hour. All obtained products were easily purified by silica gel column chromatography. Additionally, they completely soluble in polar solvent such as CH<sub>3</sub>OH and DMSO, showed less solubility in CH<sub>2</sub>Cl<sub>2</sub>, and was insoluble in water. The addition of silica gel was essential and promoted the cyclization reaction while the yield was less than 9% yield without silica gel.<sup>24,25</sup> Nevertheless, the reason behind effect of silica gel is still not clear.

The molecular structures of the cyclized products **2** were characterised by NMR, HRMS, IR, UV/Vis, and fluorescent

**Table 1** Substrate scopes<sup>a</sup>



<sup>a</sup> Reaction conditions: **1** (0.5 mmol), LiOTf (0.5 mmol), AgOTf (0.05 mmol), silica gel (1.27 g), CH<sub>2</sub>Cl<sub>2</sub> (4 mL).

spectroscopy. The  $^1\text{H}$  NMR results revealed that the imidazole ring had a lower electron density than that of bicyclic imidazo [1,2-*a*]pyridine. The chemical shifts of the CH signals in the imidazole ring (13-position of the pyridoimidazoisoquinolinium skeleton and 3-position of the imidazopyridine skeleton) shifted downfield by 0.64–0.90 ppm after cyclization.

The single-crystal X-ray diffraction results of **2b** (Fig. 2), and the values of the selected geometrical parameters (Table 2) revealed that the tetracyclic parent skeleton were virtually coplanar (mean deviation 0.069 Å) to each other. The four imidazole C–N bonds were almost identical in length and similar to the partial double bond lengths in five-membered heterocycles.<sup>26</sup> These results indicated that the imidazole moiety of the product retained the resonance characteristics of the imidazolium cation. Furthermore, the oxygen atom (O1) in trifluoromethanesulfonate, used as a counter anion, possessed a negative charge and thus interacted with the cationic **2b**. Consequently,  $\text{O}^-$  coordinated with the cationic carbon (C1) at a distance of 3.104(2) Å, where the interatomic distance was shorter than the sum of the van der Waals radii (3.25 Å).<sup>27</sup> A side-view of the crystal packing structure revealed the formation of  $\pi$ - $\pi$  stacking between the two tetracyclic planes with distances of 3.399 and 3.490 Å (Fig. 2b).

The optical properties of **2** were characterized by UV absorption and fluorescence spectroscopy in  $\text{CH}_3\text{OH}$ , and the corresponding data are shown in Fig. 3 and Table 3. These compounds exhibited trimodal absorption bands in the range of 340–375 nm. Furthermore, the absorption maxima ( $\lambda_{\text{abs}}$ ) of these compounds were not affected by the substituents at the 6-position on the tetracyclic skeleton, while the emission maxima ( $\lambda_{\text{em}}$ ) increasingly redshifted as the electron-donating nature of the substituent increased from 421 to 447 nm for **2a–e**,

Table 2 Selected atomic distances (Å)

C1–N1	1.373(2)	C3–N2	1.379(2)
C1–N2	1.372(2)	C1...O1	3.104(2)
C2–N1	1.406(2)		

respectively. Thienyl, vinyl, and alkyl substituted compounds **2f–h** exhibited emissions at 435, 438, and 419 nm, respectively. All compound has high fluorescence intensities with quantum yields ( $\Phi_{\text{F}}$ ) in the range of 39–63%. Additionally, these compounds exhibited very little solvent dependence in  $\text{CH}_2\text{Cl}_2$  as nonpolar solvent ( $\lambda_{\text{abs}} = 341$ ,  $\lambda_{\text{em}} = 425$  nm for **2c**) and HEPES buffer ( $\lambda_{\text{abs}} = 340$ ,  $\lambda_{\text{em}} = 426$  nm) (Fig. S1†).

The possibility of employing the obtained compounds in cellular imaging was then investigated. Consequently, the live human cervical cancer (HeLa) cells were incubated for 30 min with each derivative (2  $\mu\text{M}$ ). The standard 3-(4,5-dimethylthiazol-2-yl)-2,5-diphenyltetrazolium bromide (MTT) assay showed that none of the compounds **2a–h** affected cell viability under imaging conditions (Fig. S2†). The confocal laser scanning microscopic (CLSM) images revealed that the tetracyclic compounds were selectively localized in the cytoplasm without being transported into the nucleus (Fig. S3†). Additionally, autofluorescence without staining with the compounds was confirmed to be negligible. The intracellular fluorescence intensity of **2c** was the strongest, while those of the other compounds were not correlated with the fluorescent quantum yields in  $\text{CH}_3\text{OH}$  (Fig. 4). The subcellular localization of compound **2c** was investigated by colocalization microscopy techniques. The HeLa cells were treated with 2  $\mu\text{M}$  of **2c** and commercially available organelle trackers *i.e.*, MitoTracker Green, ER Tracker Green, and LysoTracker Green (Fig. 5 and

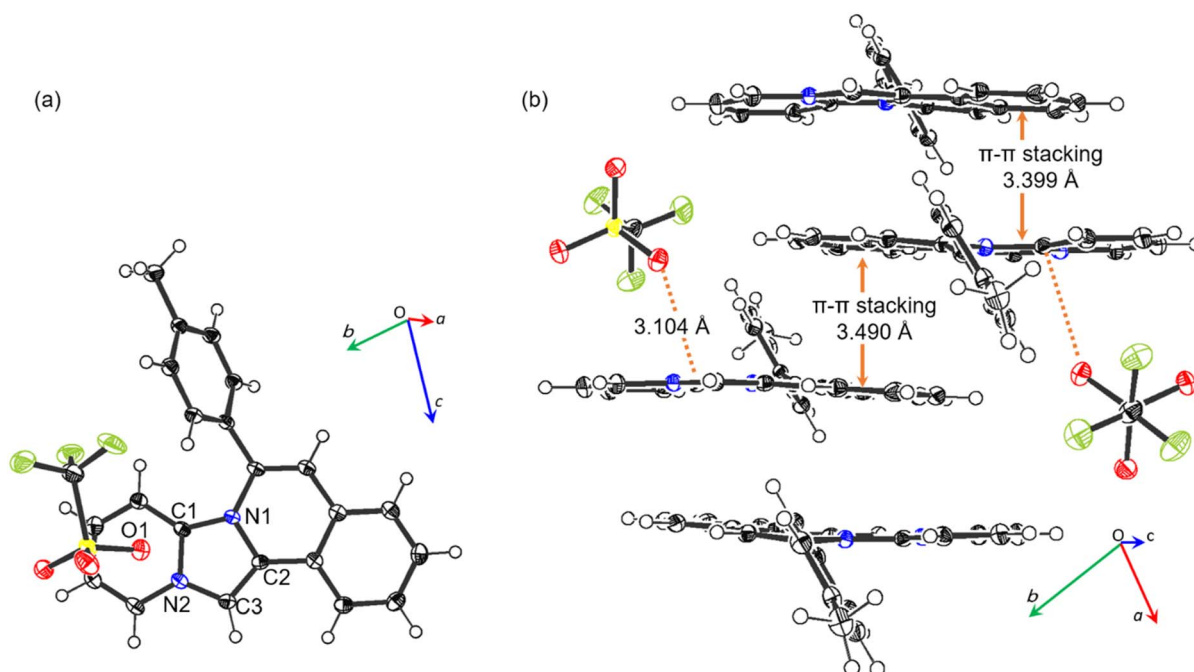


Fig. 2 Crystal structure of **2b**. (a) Top view and (b) packing structure from side view, with 50% probability thermal ellipsoids.

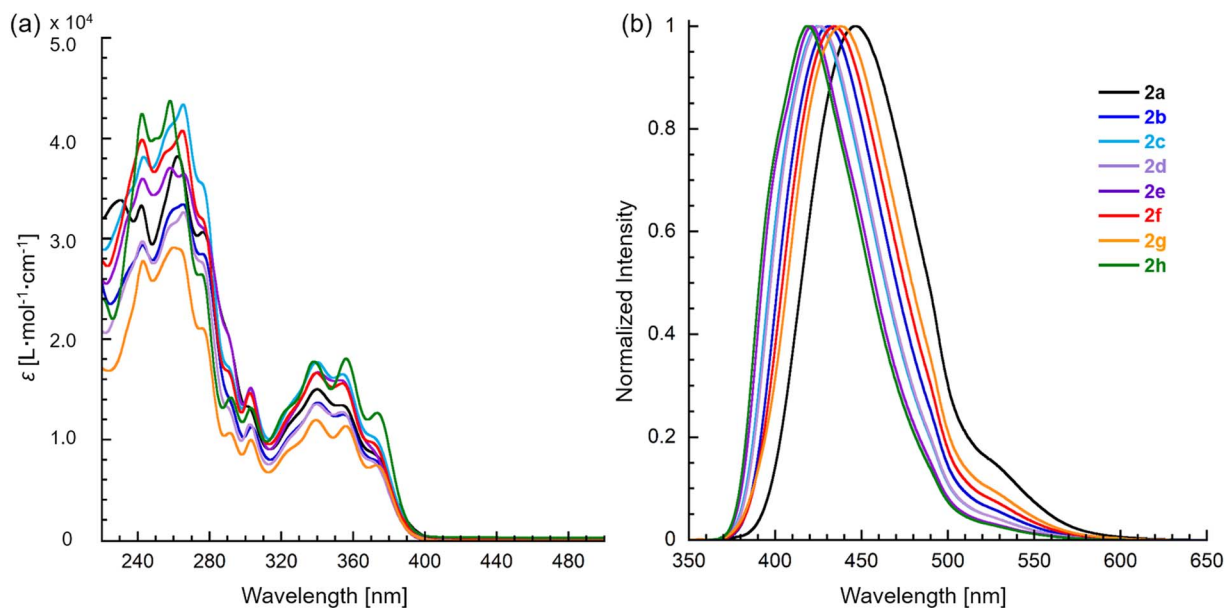


Fig. 3 (a) Absorption and (b) fluorescence spectra of pyridoimidazoisquinoliniums **2a–h** in  $\text{CH}_3\text{OH}$ . The excitation wavelength of fluorescence are at 340 nm.

Table 3 Optical properties<sup>a</sup>

Compd	R	$\lambda_{\text{abs}}$ (nm)	$\lambda_{\text{em}}^b$ (nm)	$\Phi_{\text{F}}^b$ (%)
<b>2a</b>	4- $\text{CH}_3\text{OC}_6\text{H}_4$	340	354	42
<b>2b</b>	4- $\text{CH}_3\text{C}_6\text{H}_4$	341	355	49
<b>2c</b>	$\text{C}_6\text{H}_5$	340	354	62
<b>2d</b>	4- $\text{FC}_6\text{H}_4$	340	354	49
<b>2e</b>	4- $\text{CF}_3\text{C}_6\text{H}_4$	341	353	63
<b>2f</b>	3-Thienyl	340	354	39
<b>2g</b>	1-Cyclohexenyl	340	356	43
<b>2h</b>	<i>n</i> -Butyl	338	356	63

<sup>a</sup> In  $\text{CH}_3\text{OH}$ . <sup>b</sup> Excitation at 340 nm, and quantum yield using anthracene as standard.

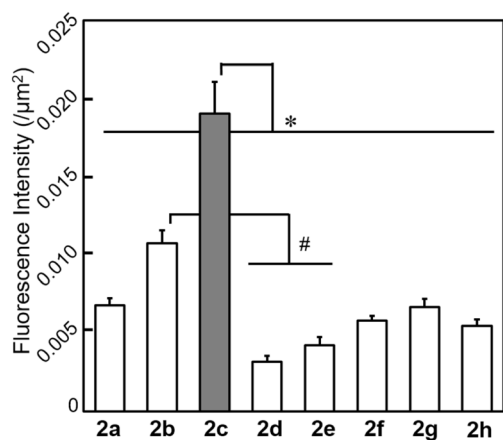


Fig. 4 Intracellular fluorescence intensity of HeLa cells incubated with **2** ( $2 \mu\text{M}$ ) for 30 min at  $37^\circ\text{C}$  detected by CLSM. Mean  $\pm$  SE,  $n = 39\text{--}40$ ,  $*p < 0.05$  relative to **2c**,  $\#p < 0.05$  relative to **2b** (Tukey–Kramer's test).

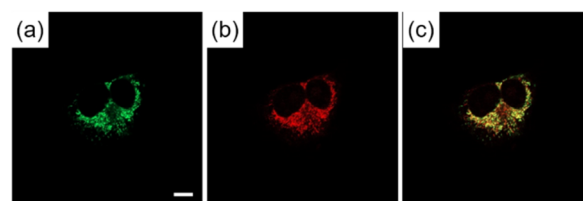


Fig. 5 CLSM images of HeLa cells incubated for 30 min with (a) MitoTracker Green ( $200 \text{ nM}$ ) for 30 min and (b) **2c** ( $2 \mu\text{M}$ ). (c) Is the merge image of (a) and (b). Scale bar:  $10 \mu\text{m}$ .

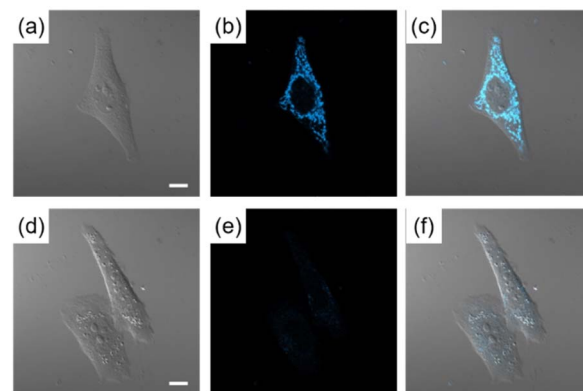


Fig. 6 CLSM images of HeLa cells incubated for (a)–(c) 30 min with **2c** ( $2 \mu\text{M}$ ), and (d)–(f) 1 h with CCCP ( $100 \mu\text{M}$ ) then 30 min with **2c** ( $2 \mu\text{M}$ ) and CCCP ( $100 \mu\text{M}$ ). (c) Is the merge image of (a) and (b). (f) Is the merge image of (d) and (e). Scale bar:  $10 \mu\text{m}$ .

$\text{S4}^\dagger$ ). Compound **2c** was localized mitochondrial specificity, unlike our previously reported pyridoimidazoisquinolinium with 5,6-disubstitutions.<sup>17</sup> Therefore we further investigated the

propulsion of localization and how it is affected upon disrupting the mitochondrial membrane potential (MMP). The intracellular fluorescence intensity of **2c** significantly decreased upon a treatment with a membrane depolarising agent, carbonyl cyanide *m*-chlorophenyl hydrazone (CCCP), which reduced the MMP (Fig. 6).<sup>28,29</sup> These results indicated that the specific localization of **2c** on the mitochondrial depended on MMP.

## Conclusion

This study reported the synthesis of novel charged heteroarenes consisting of imidazo[1,2-*a*]pyridine-fused isoquinolines from 2-(2-ethynylphenyl)imidazo[1,2-*a*]pyridines by intramolecular cyclization. The reaction proceeded with the catalytic activity of AgOTf, with LiOTf as the counter anion source and silica gel as the additive at room temperature for a short reaction times. The X-ray diffraction results revealed that pyrido[1',2';2,3]imidazo[5,1-*a*]isoquinolinium trifluoromethanesulfonate **2b** exhibited considerable planar parent tetracyclic skeletons and formed  $\pi$ - $\pi$  stacking with neighbouring molecules. In a methanol solution, the newly synthesised pyridoimidazoisoquinolinium exhibited strong fluorescence. Finally, the possible application of the obtained pyridoimidazoisoquinoliniums in cell imaging was assessed. The results revealed that the 6-phenyl derivative **2c** showed strong localized mitochondrial specificity. These result are extremely important basic knowledge for the development of cell staining agents using ionic compounds consisting of imidazopyridine skeleton. Further investigations on the wide scope of cyclization by Ag catalysts with silica gel to afford cationic heteroarenes and elucidating the intracellular-imaging mechanism are currently underway in our laboratory.

## Conflicts of interest

There are no conflicts to declare.

## Acknowledgements

This research was supported by a research grant from Institute of Pharmaceutical Life Sciences, Aichi Gakuin University and Nagai Memorial Research Scholarship from the Pharmaceutical Society of Japan (M. K.).

## Notes and references

- 1 J. Zhang, X. Chai, X.-P. He, H.-J. Kim, J. Yoon and H. Tian, *Chem. Soc. Rev.*, 2019, **48**, 683–722.
- 2 M. Gao, F. Yu, C. Lv, J. Choo and L. Chen, *Chem. Soc. Rev.*, 2017, **46**, 2237–2271.
- 3 H. Kobayashi, M. Ogawa, R. Alford, P. L. Choyke and Y. Urano, *Chem. Rev.*, 2010, **110**, 2620–2640.
- 4 X. Tian, L. C. Murfin, L. Wu, S. E. Lewis and T. D. James, *Chem. Sci.*, 2021, **12**, 3406–3426.
- 5 J. V. Jun, D. M. Chenoweth and E. J. Petersson, *Org. Biomol. Chem.*, 2020, **18**, 5747–5763.
- 6 E. Kozma and P. Kele, *Org. Biomol. Chem.*, 2019, **17**, 215–233.
- 7 L. Wang, M. S. Frei, A. Salim and K. Johnsson, *J. Am. Chem. Soc.*, 2019, **141**, 2770–2781.
- 8 J. Zhou and H. Ma, *Chem. Sci.*, 2016, **7**, 6309–6315.
- 9 Y. Tang, D. Lee, J. Wang, G. Li, J. Yu, W. Lin and J. Yoon, *Chem. Soc. Rev.*, 2015, **44**, 5003–5015.
- 10 M. Baker, *Nature*, 2010, **466**, 1137–1140.
- 11 P. Bosch, V. García, B. S. Bilen, D. Sucunza, A. Domingo, F. Mendicuti and J. J. Vaquero, *Dyes Pigm.*, 2017, **138**, 135–146.
- 12 P. Bosch, D. Sucunza, F. Mendicuti, A. Domingo and J. J. Vaquero, *Org. Chem. Front.*, 2018, **5**, 1916–1927.
- 13 P. Bosch, G. Marcelo, A. Matamoros-Recio, D. Sucunza, F. Mendicuti, A. Domingo and J. J. Vaquero, *Dyes Pigm.*, 2021, **192**, 109443.
- 14 S. Mayakrishnan, M. Tamizmani, C. Balachandran, S. Aoki and N. U. Maheswari, *Org. Biomol. Chem.*, 2021, **19**, 5413–5425.
- 15 L. Yan, W. Ma, J. Lan, H. Cheng, Z. Bin, D. Wu and J. You, *Chem. Sci.*, 2021, **12**, 2419–2426.
- 16 M. Kawakubo, Y. Inaguma, Y. Murata, M. Matsumura and S. Yasuike, *Tetrahedron Lett.*, 2022, **105**, 154054.
- 17 M. Kawakubo, Y. Inoh, Y. Inaguma, R. Kokubugata, Y. Murata, M. Matsumura, T. Furuno and S. Yasuike, *ChemistrySelect*, 2023, **8**, e202303017.
- 18 H. Zhou, W. Wang, O. Khorev, Y. Zhang, Z. Miao, T. Meng and J. Shen, *Eur. J. Org. Chem.*, 2012, **2012**, 5585–5594.
- 19 Z. Qi, S. Yu and X. Li, *J. Org. Chem.*, 2015, **80**, 3471–3479.
- 20 C. R. Nathaniel, M. Neetha and G. Anilkumar, *Appl. Organomet. Chem.*, 2021, **35**, e6141.
- 21 A. K. Clarke, H. E. Ho, J. A. Rossi-Ashton, R. J. K. Taylor and W. P. Unsworth, *Chem.-Asian J.*, 2019, **14**, 1900–1911.
- 22 G. Fang and X. Bi, *Chem. Soc. Rev.*, 2015, **44**, 8124–8173.
- 23 M. Harmata, in *Silver in Organic Chemistry*, ed. P. Belmont, John Wiley & Sons Inc, Hoboken, 2010, vol. 5, pp. 143–162.
- 24 C. M. Sharland, J. Singkhonrat, M. NajeebUllah, S. J. Hayes, D. W. Knight and D. G. Dunford, *Tetrahedron Lett.*, 2011, **52**, 2320–2323.
- 25 M. Kawakubo, H. Ohta, Y. Murata, M. Matsumura and S. Yasuike, unpublished data.
- 26 F. H. Allen, O. Kennard, D. G. Watson, L. Brammer, A. G. Orpen and R. Taylor, *J. Chem. Soc., Perkin Trans. 2*, 1987, S1–S19.
- 27 J. Emsley, in *The Elements*, Clarendon Press, Oxford, 1998.
- 28 B. S. Padman, M. Bach, G. Lucarelli, M. Prescott and G. Ramm, *Autophagy*, 2013, **9**, 1862–1875.
- 29 F. Sivandzade, A. Bhalerao and L. Cucullo, *Bio-Protoc.*, 2019, **9**, e3128.